Supporting Information

Enhancing Selectivity and Efficiency in the Electrochemical Synthesis of Adiponitrile

Daniela E. Blanco, Aaliyah Z. Dookhith and Miguel A. Modestino *

Table of Contents

Selectivity and production rate calculations

Selectivity to adiponitrile (ADN) and by-products was calculated using the following equation:

$$S_k = \frac{moles\ of\ k\ produced}{total\ moles\ of\ all\ products} \tag{1}$$

where S_k corresponds to the selectivity towards species k. The total moles of all products are calculated based on the total current passed through the system during each experimental run.

Furthermore, Faraday's law was used to correlate the current measured in each experiment with the consumption/production of species:

$$n_k = \frac{i\,t}{n\,F} \tag{9}$$

where n_i corresponds to the moles of species *k* consumed or produced, n to number of electrons involved in the reaction, i to the current in A, t to the time in s, and F to Faraday's constant.

The ADN production rate was calculated with the following equation:

$$R_{ADN} = \frac{V_{ADN}\,\rho_{ADN}}{M_{ADN}} \frac{60}{t_{electrolysis}}$$

where R_{ADN} is the production rate in g h^{-1}, V_{ADN} the volume in ml of ADN obtained at the electrolysis with the calibration curves showed in Figure S5, ρ_{ADN} corresponds to the ADN density in g cm^{-3} , M_{ADN} to the molar mass, and $t_{electrolysis}$ to the total time of electrolysis in minutes.

IR compensation calculations

All reported working electrode potentials on the manuscript accounted for the IR compensation (IR_{comp}), and reported values were calculated according to the following equation:

$$E_{WE} = E_{app} + E_{RE} - IR_{comp}$$

where E_{WE} and E_{RE} correspond to the potential at the working and reference electrode, respectively, and E_{app}

corresponds to the applied voltage. All IR drop compensations were performed after experiments were carried out.

Standard reaction potential calculations

Standard reaction potentials were calculated from Gibbs free energy values obtained from the literature.

Cathodic Half-Cell Reaction

$2AN + 2e^- + 2H_2O \rightarrow ADN + 2\ OH^-$

ΔG°AN= 191.1 KJ/mol[1-3]

ΔG°ADN= 253.31 KJ/mol[1]

$\Delta G^\circ H_2O$= -237.14 KJ/mol[4-6]

$\Delta G^\circ OH^-$= -157.2 KJ/mol[5, 7]

$$E^\circ = \frac{\Delta G^\circ{}_{rxn}}{-nF} = \frac{30990\ J/mol}{-2 \cdot 96485\ C/mol} = -0.16\ V\ \ vs\ SHE\ XXXXXXXXXXXXXXXXX$$

$$XXXXXXXXXXXXXXXXXXXXXXXXXXXXXXXXXXXXXXXXXXXXXXXXXX$$
$$XXXXXXXXXXXXXXXXXXXXXXXXXXXXXXXXXXXXXXXXXXXXXXXXXX$$
$$XXXXXXXXXXXXXXXXXXXXXXXXXXXXXXXXXXXXXXXXXXXXXXXXXX$$
$$XXXXXXXXXXXXXXXXXXXXXXXXXXXXXXXXXXXXXXXXXXXXXXXXXX$$
$$XXXXXXXXXXXXXXXXXXXXXXXXXXXXXXXXXXXXXXXXXXXXXXXXXX$$
$$XXXXXXXXXXXXXXX$$

Anodic Half-Cell Reaction

$2\ OH^- \rightarrow H_2O + \frac{1}{2}O_2 + 2e^-$

$$E^\circ = \frac{\Delta G^\circ{}_{rxn}}{-nF} = \frac{77260\ J/mol}{-2 \cdot 96485\ C/mol} = -0.4\ V\ \ vs\ SHE$$

Industrial cell configuration

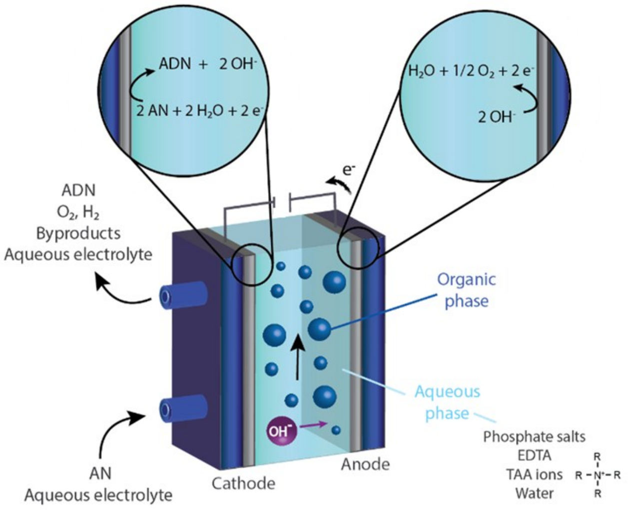

Figure S1. Industrial electrochemical cell scheme for the electrochemical hydrodimerization of AN to ADN, showing anodic and cathodic reactions, ionic flow inside the cell, organic and aqueous phases of the electrolyte, and inlet and outlet stream composition.

Uncompensated polarization curves

Figure S2 shows the polarization curve obtained for an electrolyte composed of 0.5 M Na_3PO_4, 0.03 M EDTA, and 0.02 M tetrabutylammonium hydroxide, with 0.6 M AN. While the observed current densities did not change significantly for electrolytes of varying TAA ion size, TAA ion concentration, or AN concentration (See Figure S2 in the ESI), the selectivity of the reaction was greatly affected by these parameters. The linear current density increase observed in the uncorrected polarization curves suggests that the reaction is limited by the electrolyte's ohmic resistance. This indicates that electrolyte conductivity enhancements can result in significant improvements in the efficiency of the electrochemical production of ADN.

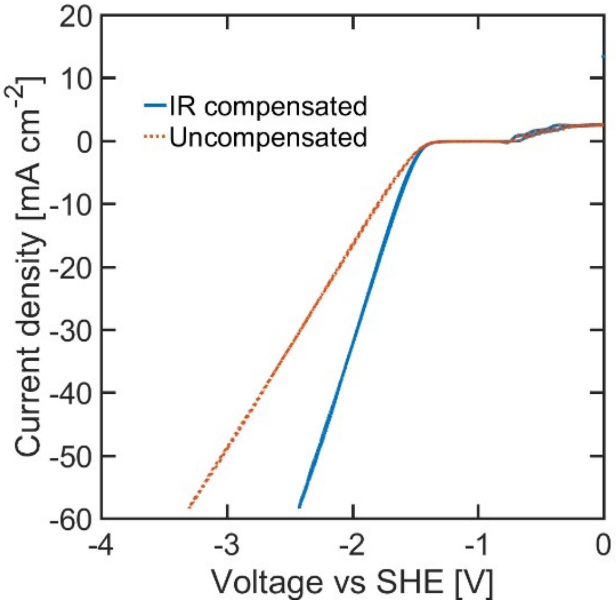

Figure S2. Cyclic voltammetry between 0 and -3.5V at 50 mV/s and the effect of IR compensation. The electrolyte contained 0.6 M AN, 0.5 M Na_3PO_4, 0.03 M EDTA, and 0.02 M TBA hydroxide. The temperature was maintained at 25°C and the pH at 11.

Cyclic Voltammetry measurements

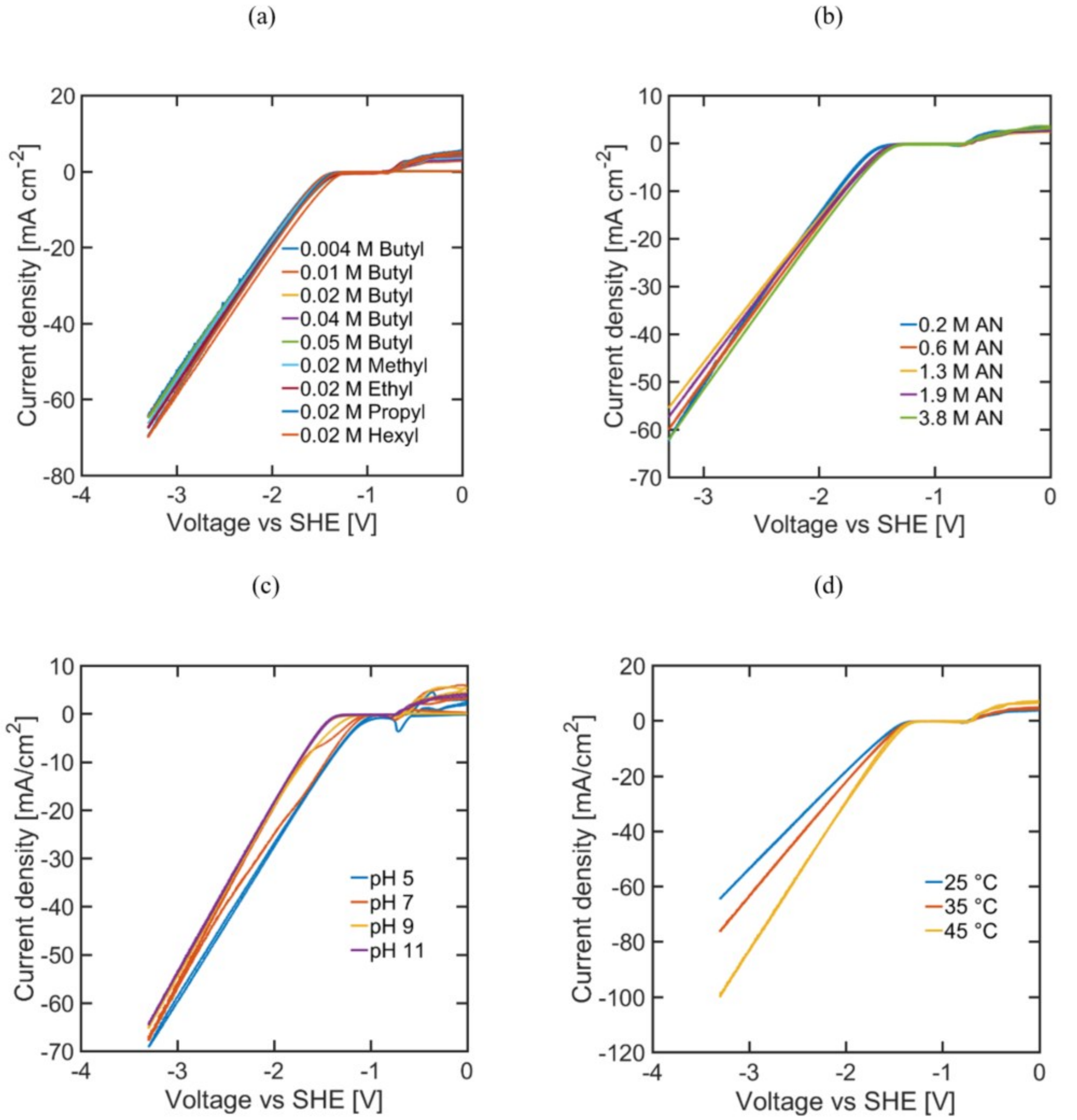

Figure S3. Cyclic voltammetry from 0 to -3.2 V vs SHE at 50 mV/s for (a) varying TAA ion size and concentration, (b) AN concentration, (c) pH, and (d) temperature. Unless specified differently, the electrolyte contained 0.6 M AN, 0.5 M Na_3PO_4, 0.03 M EDTA, and 0.02 M TBA hydroxide. The temperature was maintained at 25°C and the pH at 11.

CV and EIS measurements (see Figures S3 and S5 in the ESI) indicate that electrolyte conductivity is not significantly affected in the pH range varying from 7 to 11, reaching similar current densities. Nevertheless, slightly higher current densities are observed when pH is lower than 7, as specified in Figure 10 and Figure S2 of the ESI.

pH effects on ADN production rate

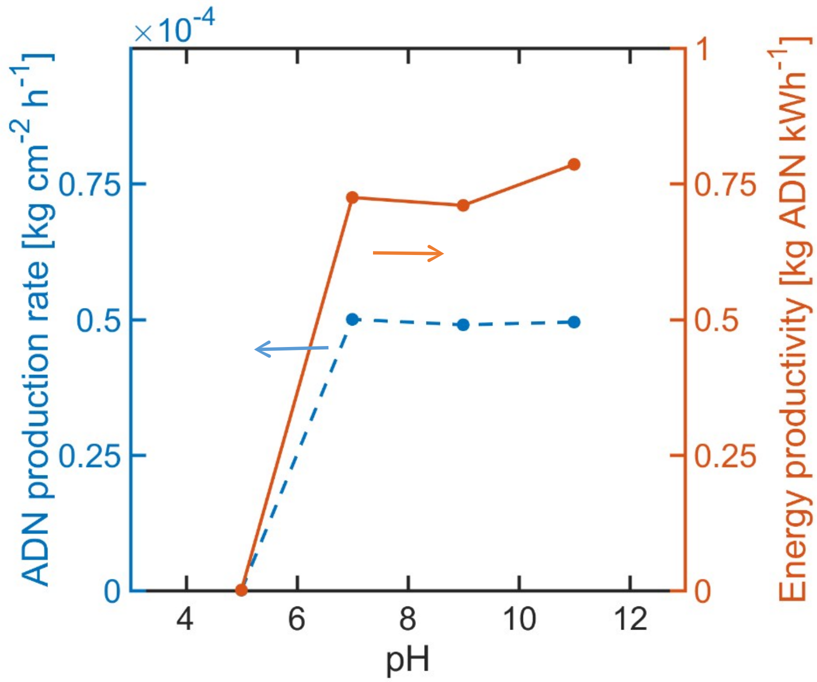

Figure S4. Adiponitrile production rate and energy conversion efficiency with varying pH at -2.1 V vs SHE. The electrolyte contained 0.6 M AN, 0.5 M Na_3PO_4, 0.03 M EDTA, and 0.02 M TBA hydroxide. The temperature was maintained at 25°C.

The production of ADN and the energy efficiency of the system drop significantly for pH lower than 7, which is due to the corresponding low selectivity towards this product.

EIS measurements


(a) (b)

Figure S5. Nyquist diagram from 7 MHz to 1 Hz and 10mV sinus amplitude for (a) varying TAA ion size and concentration, (b) AN concentration, (c) pH, and (d) temperature. Unless specified differently, the electrolyte contained 0.6 M AN, 0.5 M Na_3PO_4, 0.03 M EDTA, and 0.02 M TBA hydroxide. The temperature was maintained at 25°C and the pH at 11.

The solution resistance was obtained from the low x-intercept from a semi-circle fit on the EIS data shown above. The EIS data obtained is characteristic of two-phase systems and has already been studied for oil emulsions in water[8]. For this system, the proposed equivalent circuit consists of a resistor in parallel with a constant phase element for each time constant.

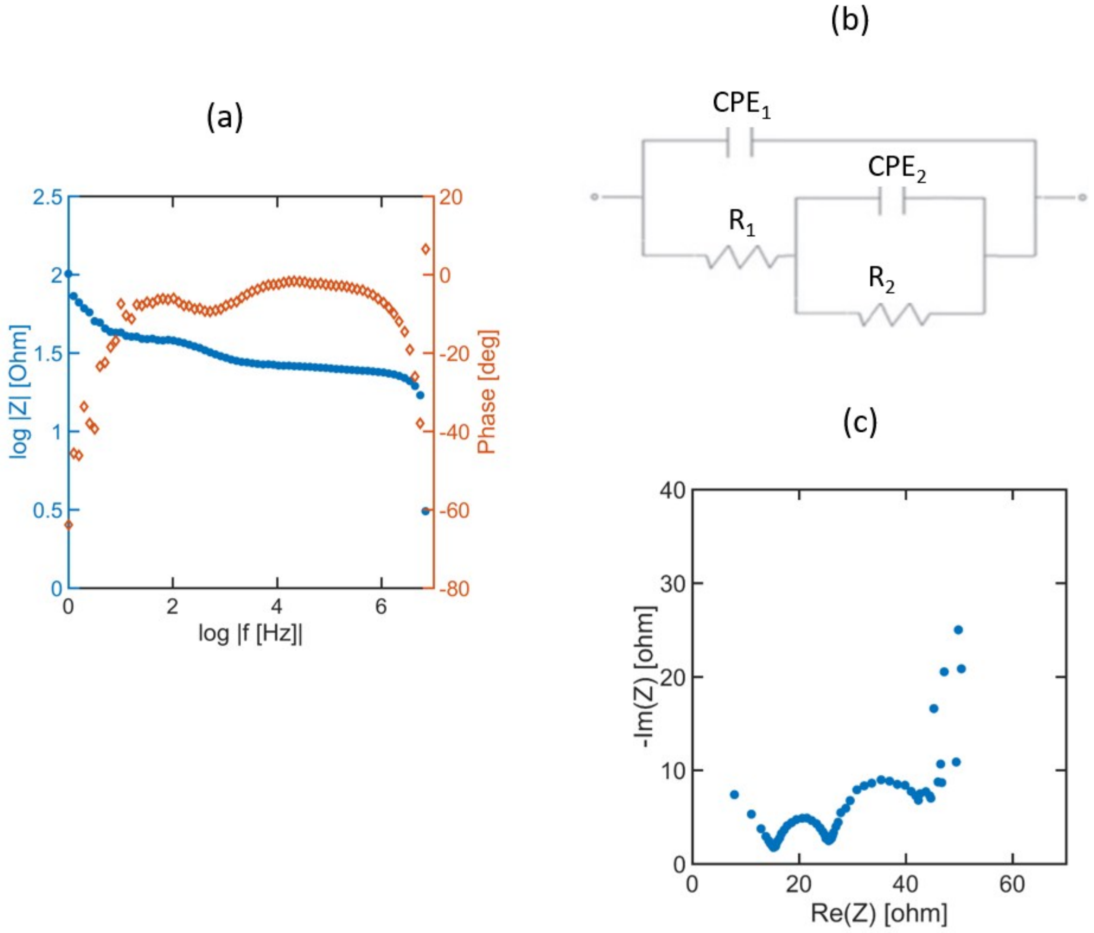

Figure S6. (a) Bode diagram, (b) proposed equivalent circuit, and (c) Nyquist plot for 10 mV sinus amplitude. The electrolyte contained 0.6 M AN, 0.5 M Na_3PO_4, 0.03 M EDTA, and 0.02 M TBA hydroxide. The temperature was maintained at 25°C and the pH at 9.

Gas chromatograph calibration curves

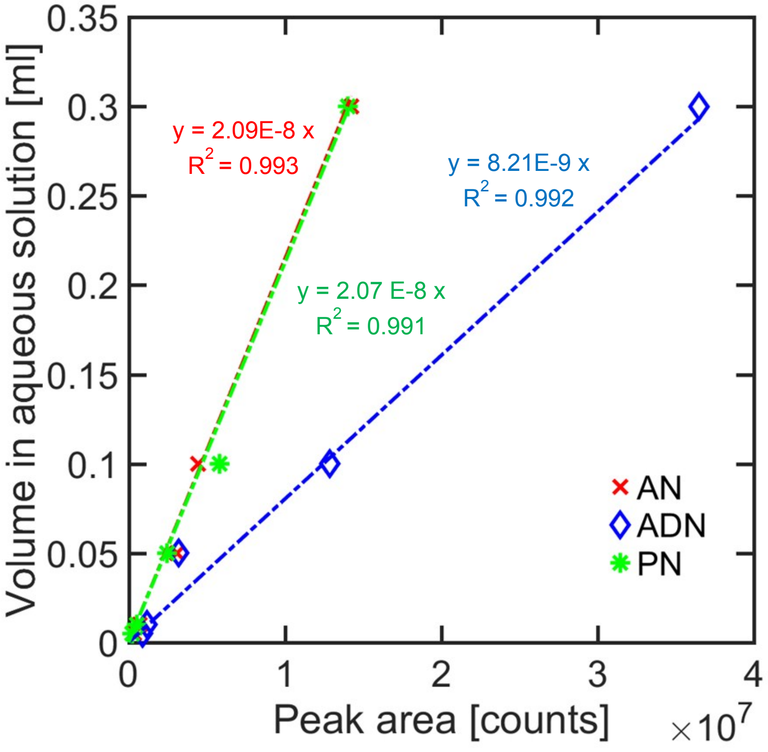

Figure S7. GC calibration curves for acrylonitrile, adiponitrile and propionitrile relating GC peak area with volume in 2 ml of electrolyte aqueous phase.

Selectivity consistency for cadmium electrode surface

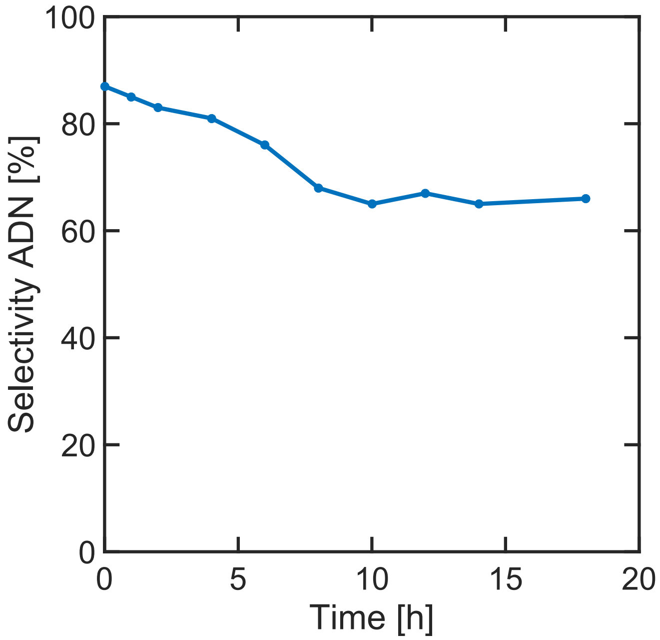

Figure S8. Variation of selectivity towards ADN with time. The electrolyte contained 0.6 M AN, 0.5 M Na_3PO_4, 0.03 M EDTA, and 0.02 M TBA hydroxide. The temperature was maintained at 25°C and the pH at 11.

The cadmium electrode surface was operated at 40 mA cm^{-2} for 10-12 hours prior to use in the experiments with catholyte solutions for consistent results in selectivity.

AN self-polymerization

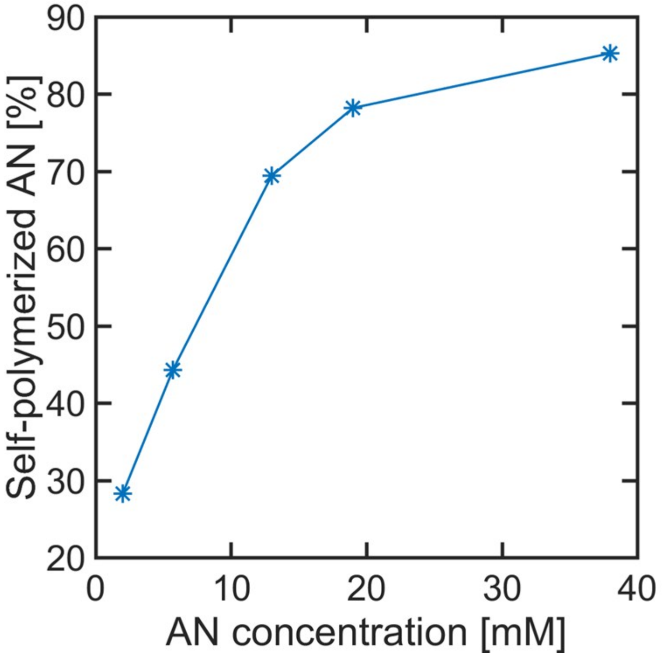

Figure S9. Fraction of bulk self-polymerized AN after 40 min with varying AN concentration. The electrolyte contained 0.5 M Na_3PO_4, 0.03 M EDTA, and 0.02 M TBA hydroxide. The temperature was maintained at 25°C and the pH at 11.

Second phase formation at high AN concentration

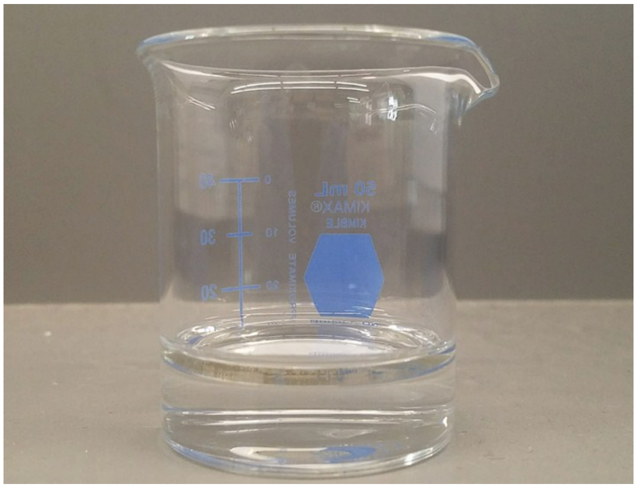

Figure S10. Second phase formation for AN concentrations above the solubility limit. The electrolyte contained 3.8 M AN, 0.5 M Na_3PO_4, 0.03 M EDTA, and 0.02 M TBA hydroxide. The temperature was maintained at 25°C and the pH at 11.

References

1. C. Yaws, P. Bajaj and H. Singh, Gibbs Energy of Formation http://chem.engr.utc.edu/ench430/2005/Teams/The-Whole/gibbs_Table.htm, (accessed July 2018).
2. M. O. Guerrero-Pérez and M. Banares, *Catal. Today*, 2015, **239**, 25–30.
3. J. Lucius, G. Olhoeft, P. Hill and S. Duke, *Properties and hazards of 108 selected substances*, U.S. Department of the Interior, 1992.
4. J. Silveira, *Sustainable Hydrogen Production Processes*, Springer International Publishing Switzerland, 2017.
5. NIST Chemistry WebBook, https://webbook.nist.gov/cgi/cbook.cgi?ID=C7732185&Units=SI&Mask=2#Thermo-Condensed, (accessed July 2018).
6. J. Vera and G. Wilczek-Vera, *Classical Theermodynamics of fluid systems*, Taylor & Francis Group, Florida, 2017.
7. J. Speight, *Lange's Handbook of Chemistry,* McGraw Hill, United States, 2005.
8. N. Perini, A. R. Prado, C. M. S. Sad, E. V. R. Castro and M. B. J. G. Freitas, *Fuel*, 2012, **91**, 224-228.